

# Experiments demonstrate that the null space of the rigidity matrix determines grain motion during vibration-induced compaction

Aline Hubbard,<sup>1</sup> Corey S. O'Hern,<sup>2,3,4</sup> and Mark D. Shattuck<sup>1,2</sup>

<sup>1</sup>*Department of Physics and Benjamin Levich Institute,  
The City College of the City University of New York, New York, 10031, USA*

<sup>2</sup>*Department of Mechanical Engineering and Materials Science,  
Yale University, New Haven, Connecticut, 06520, USA*

<sup>3</sup>*Department of Physics, Yale University, New Haven, Connecticut, 06520, USA*

<sup>4</sup>*Department of Applied Physics, Yale University, New Haven, Connecticut, 06520, USA*

(Dated: May 14, 2018)

Using a previously developed experimental method to reduce friction in mechanically stable packings of disks, we find that frictional packings form tree-like structures of geometrical families that lie on reduced dimensional manifolds in configuration space. Each branch of the tree begins at a point in configuration space with an isostatic number of contacts and spreads out to sequentially higher dimensional manifolds as the number of contacts are reduced. We find that gravitational deposition of disks produces an initially under-coordinated packing stabilized by friction on a high-dimensional manifold. Using short vibration bursts to reduce friction, we compact the system through many stable configurations with increasing contact number and decreasing dimensionality until the system reaches an isostatic frictionless state. We find that this progression can be understood as the system moving through the null-space of the rigidity matrix defined by the interparticle contact network in the direction of the gravitational force. We suggest that this formalism can also be used to explain the evolution of frictional packings under other forcing conditions.

PACS numbers: 45.70.-n, 61.43.-j, 64.70.ps, 83.80.Fg

One of the great successes of statistical mechanics is the ability to calculate the average physical properties of macroscopic systems in thermal equilibrium, e.g. atomic and molecular liquids. The microstates and probabilities with which they occur are required for determining the average properties. For example, in the microcanonical ensemble, each of the microstates at fixed energy is equally probable.

Here, we are interested in determining the structural and mechanical properties of static packings of frictional granular materials, which are collections of macroscale grains that interact via repulsive contact forces [1]. Our studies focus on *frictional* packings, which have not received as much attention as idealized packings of frictionless particles [2]. Granular packings are also strongly out-of-equilibrium since thermal fluctuations do not give rise to particle rearrangements. Grain motion is induced instead through applied external loads [3]. Moreover, the current state of the system may depend strongly on the protocol used to generate it [4–6]. In these systems, the definition of the appropriate microstates, their probabilities, and the framework for calculating average quantities is still under development [7–9].

In previous numerical simulations [12] and experimental studies [11], we showed that static packings of *frictionless* disks occur as distinct points in configuration space, whose number grows with the number of particles  $N$  in the system. We characterized each static packing using an invariant of the interparticle contact matrix and showed that static packings were not sampled with equal probabilities when generated using typical isotropic compression algorithms [12].

In recent simulations, we showed that static packings of *frictional* disks do not occur as points in configuration space, but instead as lines, areas, and higher dimensional structures (*i.e.*, geometrical families [10]) with a dimension  $m$  that grows with the difference in the number of contacts of the system from the isostatic value [13] for frictionless disks,  $m = N_c^{\text{iso}} - N_c > 0$  [10]. Thus, at each  $m$ , there are an infinite number of packings of frictional disks, but they can be classified into a finite set of geometrical families with the same contact network.

Granular systems can undergo rearrangements from one static packing to another in the presence of an applied load, *e.g.*, slow compaction during vertical tapping [14]. There have been a number of theoretical studies of slow compaction in vibrated granular packings including Tetris-like and other lattice models [15] and adsorption-desorption or parking-lot models [16], which have provided phenomenological understanding of the logarithmic relaxation of the density. Here, we seek a particle-level understanding of rearrangements that occur during vibration in terms of the motion along geometrical families and from one geometrical family to another.

In this Letter, we describe quasi-two dimensional experiments of vibrated stainless steel particles and detailed analyses of the vibration-induced particle motion. We successively applied small amplitude, high frequency vibration bursts to the packings to break interparticle contacts and induce small-scale particle rearrangements. Using accurate particle tracking techniques, we monitored changes in the interparticle contact network as the system evolved from dilute to more dense packings during

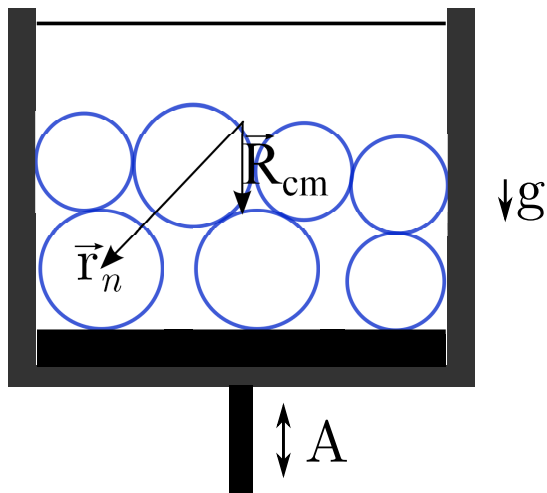


FIG. 1: (Color online) Sketch of the quasi-two dimensional vibration cell that contains a packing of seven bidisperse thin cylinders (4 small and 3 large with diameter ratio 1.246) with 11 contacts. The amplitude of the vertical vibrations is indicated by  $A$  and gravity is directed downward.  $\vec{R}_{cm}$  and  $\vec{r}_n$  locate the center of mass of the packing and position of the  $n$ th particle.

the vibrations. We found two key results: 1) The packings that occur during the compaction process are not randomly distributed in configuration space, instead they form connected lines or ‘geometrical family trees’, which verifies our previous simulation results [10]. 2) The motion of the grains during the compaction process occurs in the null space of an under-coordinated rigid link network [17] formed by the interparticle contacts. In particular, the particle motion can be accurately predicted by projecting the direction of the gravitational force onto the null space.

We performed quasi-two dimensional experiments of vibrated granular materials as shown in Fig. 1. The vibration cell has width  $L_x = 5.33$  cm, height  $L_y > 5$  cm, and thickness  $L_z = 0.34$  cm and contained  $N = 7$  bidisperse stainless steel cylinders (4 small and 3 large with diameters  $\sigma_s = 1.26$  cm and  $\sigma_l = 1.57$  cm, masses  $m_s = 2.8$  g and  $m_l = 4.3$  g, and thickness 0.32 cm). We focused on systems with a small number of grains so that we can enumerate most of the geometrical family trees during compaction. The vibration cell is formed by two plastic side walls, two glass plates, and a movable piston on the bottom. The diameter of each cylinder is a factor of 4 larger than its thickness, which ensures that the cylinder axes are always parallel to each other and perpendicular to the direction of gravity. The piston is connected to a computer controlled electromagnetic shaker that vibrates the bottom boundary.

For the experimental protocol, we first randomize the initial positions of the cylinders by applying high amplitude and low frequency (50 Hz) vibrations for one second and allow them to settle to a frictionally stabilized packing. We then periodically apply small amplitude, high

frequency (440 Hz) vibration bursts, each with duration 10 ms. The acceleration from these bursts causes the contacts between the cylinders (and between the cylinders and walls) to break, which temporarily removes the frictional forces between particles. After each burst, the system settles under gravity, contacts reform, and the system forms a new static packing. Over a series of bursts the system compacts and the number of contacts grows on average, terminating on a ‘frictionless’ packing with  $N_c = N_c^{iso} = 2N = 14$  contacts for systems with fixed boundaries and gravity. We analyzed 6901 initial packings without rattler particles on the bottom boundary and applied 20 vibration bursts to each. After roughly 15 bursts, these systems converged to 979 distinct frictionless packings.

We imaged the system with a digital camera using backlighting. We recorded images of the system after waiting 0.5 s following each burst. We tracked the positions of the cylinders with a spatial resolution of  $6 \times 10^{-6} \sigma_s$  in both the horizontal and vertical directions [18].

In Fig. 2 (a), we show the evolution of the center of mass  $\vec{R}_{cm}$  and contact number for a set of packings that compacts to a particular frictionless packing with  $N_c^{iso}$  contacts. Mechanically stable frictional packings with fixed boundaries and gravity can occur in the range  $(3N - 1)/2 \leq N_c \leq 2N$  [19, 20] or  $10 \leq N_c \leq 14$  for  $N = 7$ . The system is initialized in a dilute packing with  $N_c = 11 < N_c^{iso}$ . The center of mass evolves smoothly until the packing becomes mechanically unstable, and a new contact network is formed, in this case with  $N_c = 12$ . The  $N_c = 12$  contact network smoothly evolves until it becomes unstable, and a new interparticle contact forms with  $N_c = 13$ . The evolution of the center of mass along a geometrical family is continuous as long as the contact network remains the same. Changes in the contact network are signaled by abrupt changes in the direction of motion of the center of mass. Since we apply small amplitude vibrations, the evolution of the center of mass terminates on a frictionless packing with  $N_c^{iso}$  contacts.

When the system is initialized in a different packing, it can evolve to the same frictionless packing in Fig. 2 (a) or another one. In Fig. 2 (b), we show the geometrical family tree that leads to the frictionless packing shown in Fig. 2 (a). Note that the center of mass approaches that of the frictionless packing only along particular directions in configuration space. In Fig. 2 (c), we show the centers of mass of all packings found in the experiments. Note that the most probable packings tend to be the most compact.

We now describe a method to quantitatively predict the particle motion that occurs during the compaction process. The center of mass motion is characterized by smooth evolution while the contact network is fixed, punctuated by abrupt changes in direction when the contact network changes. While the contact network is fixed, we model the system by a network of rigid links between contacting particles. Since  $N_c^{iso} - N_c = m \geq 0$ , the

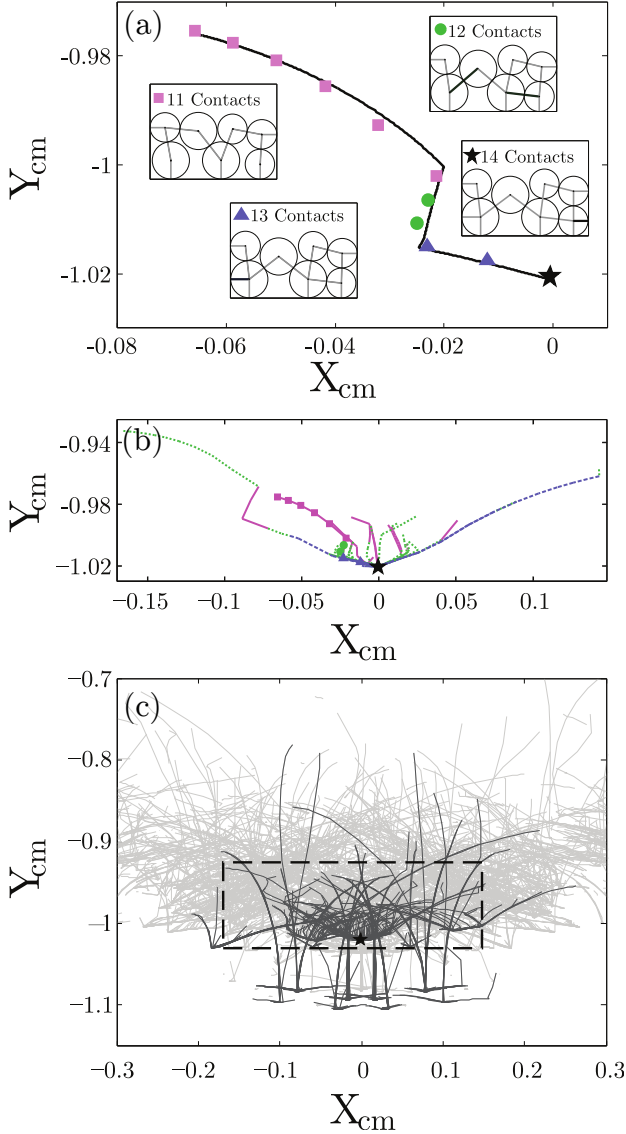


FIG. 2: (Color online) (a) Evolution of the center of mass ( $X_{\text{cm}}, Y_{\text{cm}}$ ) as the system compacts and the contact number increases from  $N_c = 11$  to 14. The star indicates a frictionless packing with  $N_c^{\text{iso}} = 14$  contacts. Snapshots of this ‘geometrical family tree’ are included for each value of  $N_c$ . The solid line shows the solution of Eq. 4 in the overdamped limit for each of the contact networks. (b) Evolution of the centers of mass for all family trees (different line types) that terminate on the frictionless packing in (a). (c) All family trees found in the vibration experiments. The family trees with probability greater than 0.6% are shaded black, while the others appear gray. The dashed rectangular region indicates the area shown in (b).

$2N \times 2N$  rigidity matrix  $K$  will possess  $m$  floppy eigenmodes  $\mathbf{e}^i = \{e_{x1}^i, e_{y1}^i, \dots, e_{xN}^i, e_{yN}^i\}$  that form the null space and  $2N - m$  non-floppy modes [17]. Each contact network will possess a different rigidity matrix and set of null-space modes. We define the rigidity matrix and its eigenmodes  $\mathbf{e}_{s,n}^i$  for each experimental packing, where the

subscripts  $s$  and  $n$  indicate the initial condition and vibration burst number, respectively. We have shown previously that vibrations release the frictional contacts [11]. We now hypothesize that the release of friction induces motion in the null space along directions that do not cost energy, and thus frictional packings live in the null space.

To test whether the particle motion is confined to the null space, we calculate the normalized difference between the total particle motion and the motion that occurs in the null space,

$$W_{s,n} = \frac{(\Delta \mathbf{r}_{s,n})^2 - \sum_{i=1}^m (\Delta \mathbf{r}_{s,n} \cdot \mathbf{e}_{s,n}^i)^2}{(\Delta \mathbf{r}_{s,n})^2}, \quad (1)$$

where  $\Delta \mathbf{r}_{s,n} = \mathbf{r}_{s,n+1} - \mathbf{r}_{s,n}$  and  $\mathbf{r}_{s,n}$  is the  $2N$ -dimensional vector that gives the positions of the particles for initial condition  $s$  and burst  $n$ .  $W_{s,n} = 0$  indicates that all particle motion is confined to the null space. In Fig. 3 (a), we plot the cumulative distribution  $C(W_{s,n})$ , which shows that 99% of the particle motions satisfy  $W_{s,n} \lesssim 10^{-3}$ . Thus, nearly all of the particle motion during compaction is confined to the null space.

To complete our theoretical analysis of vibration-induced compaction, we further hypothesize that particle motion occurs in the direction of gravity projected onto the null space. We now compare the direction of motion in configuration space during compaction to the direction of the gravitational force decomposed onto the null space,

$$\mathbf{G}_{s,n} = \sum_{i=1}^m [\mathbf{e}_{s,n}^i \cdot (-\mathbf{g})] \mathbf{e}_{s,n}^i, \quad (2)$$

where  $\mathbf{g} = \{0, m_s g, \dots, 0, m_l g\}$  is a  $2N$ -dimensional vector with a zero for the  $x$ -component and the gravitational force for the  $y$ -component for each particle. The degree to which the particle displacements track the direction of gravity can be determined by calculating the normalized overlap between  $\mathbf{G}_{s,n}$  and  $\Delta \mathbf{r}_{s,n}$ . To measure the deviation from complete overlap, we define

$$\alpha_{s,n} = 1 - \frac{\mathbf{G}_{s,n} \cdot \Delta \mathbf{r}_{s,n}}{|\mathbf{G}_{s,n}| |\Delta \mathbf{r}_{s,n}|}. \quad (3)$$

$\alpha_{s,n} = 0$  indicates that a given displacement  $\Delta \mathbf{r}_{s,n}$  is aligned with the direction of gravity in the null space. In Fig. 3 (b), we plot the cumulative distribution  $C(\alpha_{s,n})$ , which shows that 99% of the particle motions satisfy  $\alpha_{s,n} \lesssim 10^{-3}$ . Thus, nearly all of the particle displacements are in the direction of gravity in the null space. However, a few displacements out of  $10^5$  possess  $\alpha_{s,n} \sim 1$  (with overlap angles greater than  $30^\circ$ ) indicated by the small peak in the probability distribution  $P(\alpha_{s,n})$  in the inset to Fig. 3 (b). These few instances of large  $\alpha_{s,n}$  are caused by two effects: 1) The vibration bursts were not large enough to break some of the frictional contacts between particles and the bottom wall. In which case, these particles did not move in the direction of gravity in the null space. These occurrences of large  $\alpha_{s,n}$  can

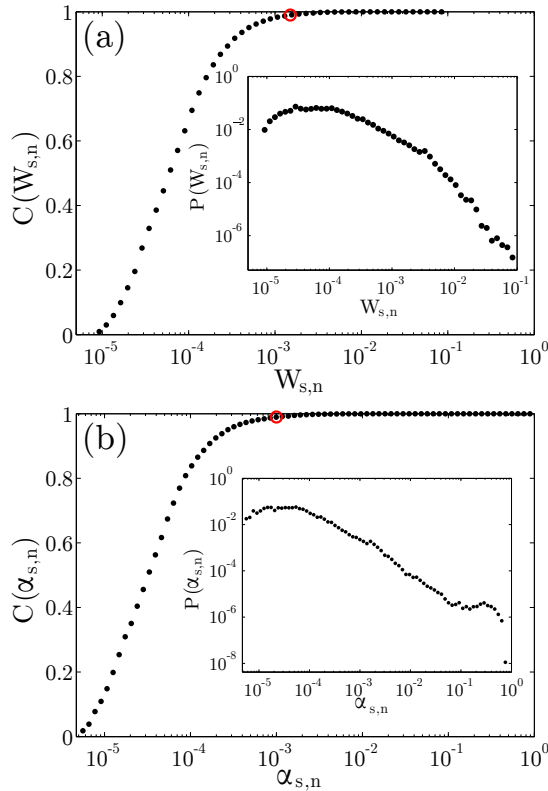


FIG. 3: (Color online) (a) Cumulative distribution  $C(W_{s,n})$  of the normalized differences  $W_{s,n}$  between the particle motion and the motion that occurs in the null space for each initial condition  $s$  and vibration burst  $n$ . (See Eq. 1.) The open red circle indicates that 99% of the projections satisfy  $W_{s,n} \lesssim 10^{-3}$ . The inset shows the probability distribution  $P(W_{s,n})$ . The minimum  $W_{s,n} \sim 10^{-5}$  is set by the resolution of the particle tracking. (b) Cumulative distribution  $C(\alpha_{s,n})$  of the deviations from complete overlap  $\alpha_{s,n}$  between the particle displacements and direction of gravity for each  $s$  and  $n$ . The open red circle indicates that 99% of the overlaps satisfy  $\alpha_{s,n} \lesssim 10^{-3}$ . The inset shows the probability distribution  $P(\alpha_{s,n})$ .

be removed by increasing the amplitude of the vibration or by adding constraints to the rigidity matrix to represent frictional contacts. 2) The particle positions in the packing are such that different subsequent particle motions are equally likely. For example, when a particle falls vertically downward on top of another particle. Whether the particle moves downward and to the right or to the left is sensitive to the precise horizontal location of the top particle. Once the direction of motion in configuration space is chosen,  $\alpha_{s,n}$  is nearly zero during subsequent evolution.

We also solved for the full particle trajectories using

the instantaneous rigidity matrices obtained from experiments by numerically solving Newton's equations of motion for the configuration space vector  $\mathbf{r}$ :

$$M \frac{d^2 \mathbf{r}}{dt^2} = -K \mathbf{r} - b \frac{d\mathbf{r}}{dt} - \mathbf{g}, \quad (4)$$

where  $M$  is the mass matrix and  $b$  is the damping parameter. We solved Eq. 4 in the overdamped limit, *i.e.*,  $d\mathbf{r}/dt = -K\mathbf{r}/b - \mathbf{g}/b$ , and find that the simulations are able to accurately recapitulate the full particle trajectories in the experiments as shown by the solid line in Fig. 2 (a).

We performed quasi-two dimensional experiments of granular materials undergoing vibration-induced compaction. Using accurate particle tracking techniques, we monitored the motion of all grains in the system following successive vibration bursts. Using the center of mass to classify the static packings, we find that they are organized into geometrical families. Abrupt changes in the direction of the evolution of the family in configuration space signal changes in the contact network. These experimental results represent a breakthrough in our understanding frictional granular packings and confirm recent simulations that identified geometrical families in isotropically compressed frictional packings [10]. We also modeled each contact network using rigid links between contacting grains and showed that grain motion between vibration bursts occurs in the null space of the under-coordinated rigidity matrix. More specifically, we find that the particles move in the direction of gravity projected into the null space. This novel method for determining particle motion can be applied to other driving mechanisms, *e.g.* fixed applied shear stress, and will allow us to understand shear-induced jamming and protocol-dependent mechanical properties in frictional packings.

### Acknowledgments

We acknowledge financial support from the W. M. Keck Foundation Grant No. DT061314 (C.S.O.) and the National Science Foundation (NSF) Grant No. DMR-0934206 (A.H. and M.D.S.). We also acknowledge support from the Kavli Institute for Theoretical Physics (through NSF Grant No. PHY-1125915), where some of this work was performed. This work also benefited from the facilities and staff of the Yale University Faculty of Arts and Sciences High Performance Computing Center and the NSF (Grant No. CNS-0821132) that in part funded acquisition of the computational facilities.

- Phys.* **1** (2010) 347.
- [3] M. Nicolas, P. Duru, and O. Pouliquen, *Eur. Phys. J. E* **3** (2000) 309.
  - [4] S. Torquato, T. M. Truskett, and P. G. Debenedetti, *Phys. Rev. Lett.* **84** (2000) 2064.
  - [5] P. Chaudhuri, L. Berthier, and S. Sastry, *Phys. Rev. Lett.* **104** (2010) 165701.
  - [6] C. F. Schreck, C. S. O'Hern, and L. E. Silbert, *Phys. Rev. E* **84** (2011) 011305.
  - [7] S. F. Edwards and R. B. S. Oakeshott, *Physica A* **157** (1989) 1080.
  - [8] S. Henkes and B. Chakraborty, *Phys. Rev. E* **79** (2009) 061301.
  - [9] K. Wang, C. Song, P. Wang, and H. A. Makse, *Phys. Rev. E* **86** (2012) 011305.
  - [10] T. Shen, S. Papanikolaou, C. S. O'Hern, and M. D. Shattuck, *Phys. Rev. Lett.* **113** (2014) 128302.
  - [11] G.-J. Gao, J. Blawdziewicz, C. S. O'Hern, and M. D. Shattuck, *Phys. Rev. E* **80** (2009) 061304.
  - [12] G. J. Gao, J. Blawdziewicz, and C. S. O'Hern, *Phys. Rev. E Phys. Rev. E* **74** (2006) 061304.
  - [13] R. Blumenfeld, *New J. Phys.* **9** (2007) 160.
  - [14] E. R. Nowak, J. B. Knight, E. Ben-Naim, H. M. Jaeger, and S. R. Nagel, *Phys. Rev. E* **57** (1998) 1971.
  - [15] E. Caglioti, V. Loreto, H. J. Herrmann, and M. Nicodemi, *Phys. Rev. Lett.* **79** (1997) 1575.
  - [16] J. Talbot, G. Tarjus, and P. Viot, *Eur. Phys. J. E* **5** (2001) 445.
  - [17] D. J. Jacobs and M. F. Thorpe, *Phys. Rev. E* **53** (1996) 3682.
  - [18] M. D. Shattuck, "Experimental Techniques" in *Handbook of Granular Materials*, Eds. S. V. Franklin and M. D. Shattuck (CRC Press, Boca Raton, 2015).
  - [19] K. Shundyak, M. van Hecke, and W. van Saarloos, *Phys. Rev. E* **75** (2007) 010301(R).
  - [20] S. Papanikolaou, C. S. O'Hern, and M. D. Shattuck, *Phys. Rev. Lett.* **110** (2013) 198002.